**Special Issue**
***"Progress of Theoretical and Computational Biophysics"***

**Vol. 16, pp. 466–472 (2019)**
**doi: 10.2142/biophysico.16.0_466**

**Biophysics and Physicobiology**

https://www.jstage.jst.go.jp/browse/biophysico/

***Regular Article***

# Polymer brush in articular cartilage lubrication: Nanoscale modelling and simulation

Nobuhiko Kajinami and Mitsuhiro Matsumoto

*Department of Mechanical Engineering and Science, Graduated School of Engineering, Kyoto University, Kyoto 615-8540, Japan*

Received July 2, 2019; accepted September 17, 2019

**Human knee joints move smoothly under high load conditions due to articular cartilage and synovial fluid. Much attention is paid to the role of proteoglycans. It is suggested that a part of proteoglycan forms aggregate on the cartilage surface, making a polymer brush, which has an important role in lubrication. In order to examine the lubrication mechanism in detail, we constructed a full atom model of a polymer brush system, and carried out a series of molecular dynamics simulations to analyze its frictional properties under constant shear. We use chondroitin 6-sulfate molecules grafted on resilient surface as the polymer brush and water with sodium ions as the synovial liquid. In the steady state, polymers have large deformation and the flow of synovial fluid becomes deviate from the Coutette flow, leading to a drastic reduction of friction. Longer chains have larger reduction.**

**Key words:** articular cartilage, lubrication, polymer brush, molecular dynamics simulation

Molecular simulations have been widely used in various fields of science and engineering. In particular, they provide indispensable tools in biophysics and biochemistry to examine dynamic process at atomic scales. In this paper, we present our molecular simulation study for lubrication mechanism of articular cartilage, as an example in biomechanics application.

Human joints move very smoothly even under high load, owing to articular cartilages covering each tip of the bones [1]. The relevant part of the articular cartilage, extracellular matrix, is a composite of collagen fibers, proteoglycan, and hyaluronic acid. The dynamic friction coefficient between two articular cartilage plates was found to be as small as 0.002–0.020 [2]. The lubrication mechanism has been discussed from various viewpoints [3,4] in order to develop better joint replacements. Two relevant mechanisms are proposed; fluid pressurization mediated lubrication [5] and boundary lubrication due to biopolymers [6,7].

We are investigating the role of biopolymers. On the surface of cartilages, aggregates of proteoglycan, negatively charged glycosylated protein, form a polymer brush. The role of such ionic polymer brush in lubrication has been theoretically pointed out [8], and we have carried out a series of molecular dynamics (MD) simulation with a coarse-grained model [9]. However detailed mechanism at atomic scale has not been fully understood.

Here we carry out full atom MD simulations with a nanoscale model of ionic polymer brush. One of our interests exists in the effect of various control parameters, such as

Corresponding author: Nobuhiko Kajinami, Department of Mechanical Engineering and Science, Graduated School of Engineering, Kyoto University, Kyoto-daigaku Katsura C3, Kyoto 615-8540, Japan.
e-mail: kajinami.nobuhiko.82a@st.kyoto-u.ac.jp

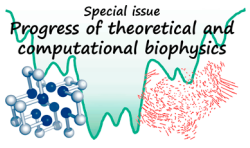


◀ ***Significance*** ▶

Full atom modelling and molecular dynamic simulations of ionic polymer systems are presented to investigate lubrication mechanism of articular cartilage, as an example of molecular simulation study in biomechanics. We use chondroitin 6-sulfate molecules grafted on resilient surface as the polymer brush and water with sodium ions as the synovial liquid. With this model, we carried out a series of molecular dynamics simulation and analyzed how polymer brush and synovial fluid affect the lubrication under constant shear. Polymers have large deformation and the flow of synovial fluid becomes deviate from the Coutette flow, leading to a drastic reduction of friction.

shear rate and polymer length. In this paper, preliminary results of the simulation under a limited parameter range are described to show how this type of full atom simulations is utilized in the field of biotribology.

## Methods

### Molecular dynamics simulation

The simulations were performed with the LAMMPS code [10]. The equation of motion for each atom is integrated using the Verlet algorithm with a time step of 0.2 fs, and the particle-particle-particle-mesh (PPPM) method [11] was used for the electrostatic interactions. We adopt the DREIDING force field [12] for the polymer brush model. This force field is widely used for full atom simulation of various molecular systems; in particular, structure and mechanical properties of organic molecules in aqueous solutions, e.g., membranes [13] and hydrogels [14,15], have been successfully investigated with DREIDING. The original parameter set is used without any adjustment since no experimental data are available on the detailed steric structure of proteoglycan aggregates. The force field is sufficient for our purpose to investigate the lubrication properties during polymer deformation under a large shear field.

The typical energy function is

$$E_{\text{total}} = \sum_{\text{bonds}} K_r(r-r_0)^2 + \sum_{\text{angles}} K_\theta[\cos\theta - \cos\theta_0]^2 + \sum_{\text{torsions}} K_\varphi[1+\cos(n\varphi - d)] + \sum_{i<j}\left[4\varepsilon_{ij}\left\{\left(\frac{\sigma_{ij}}{r_{ij}}\right)^{12} - \left(\frac{\sigma_{ij}}{r_{ij}}\right)^{6}\right\} + \frac{Q_iQ_j}{4\pi\varepsilon_0 r_{ij}}\right] \quad (1)$$

where the total potential energy $E_{\text{total}}$ is expressed as the sum of bond stretch energy, bond angle energy, dihedral angle energy, and the non-bonding interactions. The last term consists of the van der Waals (Lennard-Jones, LJ) interaction and the electrostatic one between atom $i$ and $j$. For the water molecules, we use the TIP3P model [16], where partial charge is allotted to each atom (O and H) while only the oxygen atoms have the LJ interaction. For the LJ interaction between different species A and B, the Lorentz-Berthelot empirical rule is assumed, as

$$\varepsilon_{\text{AB}} = \sqrt{\varepsilon_{\text{AA}}\varepsilon_{\text{BB}}}, \qquad \sigma_{\text{AB}} = \frac{\sigma_{\text{AA}} + \sigma_{\text{BB}}}{2} \quad (2)$$

### Simulation model

We assume a simple polymer brush system in a rectangular box. The system consists of three components, i.e., articular cartilage surface on the top and the bottom of the box, polymer brush on each surface, and synovial fluid between the surfaces. Periodic boundary is assumed along horizontal directions ($x$ and $y$).

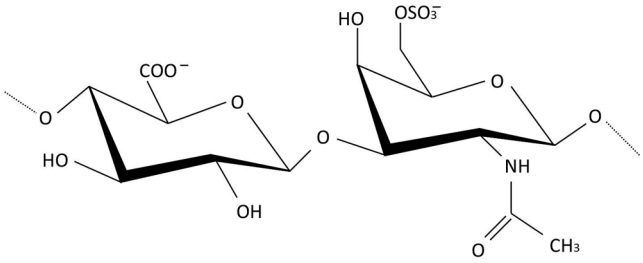


**Figure 1** A unit of chondroitin 6-sulfate.

*Polymer brush*

In a real articular cartilage system, polymer brush is composed of proteoglycan complex [17]. Since full atom simulation of the whole complex is out of reach, we investigate a component (glycosaminoglycan, GAG), which is bound to the core protein. The spacing of GAGs on the core protein is 20–40 A [18], from which we determine the area density of our brush model.

We adopt chondroitin 6-sulfate, the most important component of GAG, as the polymer, which is the majority among negatively charged polymers in articular cartilage [19]. Each unit of chondroitin 6-sulfate has two anionic sites, as shown in Figure 1. To investigate the effect of polymer length on frictional behavior, three models with different polymer length (12–75 A) are used; however, the length is still much shorter than the real GAGs (200–600 A).

We graft nine polymers as a square lattice on the top and the bottom walls of 73.6×73.6 A$^2$; the end atom (O) is connected to a fixed point on the wall by a harmonic spring in order to model resilient cartilage surface.

*Synovial fluid*

Synovial fluid is composed of various ingredients, such as hyaluronic acid and glycoprotein [20]. In this study, however, only water is used as a starting point. To keep the charge neutrality, sodium ions are added, the interaction parameters of which are taken from Ref. [21]. Effects of extra electrolytes and biopolymers are to be investigated in future.

*Articular cartilage surface*

Since articular cartilage consists mainly of water (60–85 weight% [22]), we embed water molecules in the polymer-grafted cartilage surface; 639 molecules are connected to each wall by harmonic springs to model the surface resilience. In the following description, the gap distance is defined as the distance between the two water-embedded surfaces. To prevent other atoms from passing through the surface during the simulation, extra walls are set behind the surface, which are interacting with atoms via the LJ (9-3) potential.

*Simulation procedure*

As the initial conditions, we prepare a sufficiently large simulation box with vertically elongated polymers with low water density. The system is pressurized by reducing the

**Table 1** Simulation system

| | Number of polymer units | Molecular weight [–] | Number of $Na^+$ | Number of water molecules | Number of atoms | Gap distance [A] |
|---|---|---|---|---|---|---|
| Model 0 | – | – | – | 11300 | 33900 | 35.0 |
| Model 1 | 1 | 443.34 | 36 | 2160 | 11142 | 9.0 |
| Model 2 | 4 | 1773.35 | 144 | 3750 | 18396 | 19.0 |
| Model 3 | 8 | 3516.70 | 288 | 5600 | 27258 | 35.0 |

gap distance and thermally equilibrated at 298 K with the Nosé-Hoover thermostat scheme. The final gap distance $L$ is empirically determined so that the mean pressure is similar for the three models. We adopt a rather high mean pressure of ~10 GPa to suppress the fluctuations in stress calculation. The system description is given in Table 1. A snapshot of Model 2 at equilibrium is shown in Figure 2. As a reference, we executed a similar simulation for the system without polymers (Model 0).

As the main calculation, we slide the top surface horizontally to the $y$ direction at constant speed $v_0$; in the following, results with $v_0$=500 m/s are mainly described. Also in the main calculation, the temperature is controlled to 298 K to suppress the viscous heating; the local temperature is evaluated from the atomic velocities after subtracting the macroscopic shear flow velocity.

## Results and Discussion

In equilibrium, grafted polymers are entangled in thin gaps, as shown in Figure 2. As the sliding proceeds, the entanglement is gradually relaxed and the polymers become elongated to the shear direction (Fig. 3).

In the following, properties relevant to lubrication behaviour are shown mainly in the steady state.

### Stress evaluation

To evaluate the friction, we measure the stress on the bottom surface, $\sigma_{zz}$ for pressure normal to the surface and $\sigma_{zy}$ for the shear stress. Results are shown in Figure 4 for Model 2 and Model 3, where the sliding starts at time=0. As the sliding starts, molecules (water as well as polymers) exert recovery force on the surface, leading to the $\sigma_{zy}$ increase. The

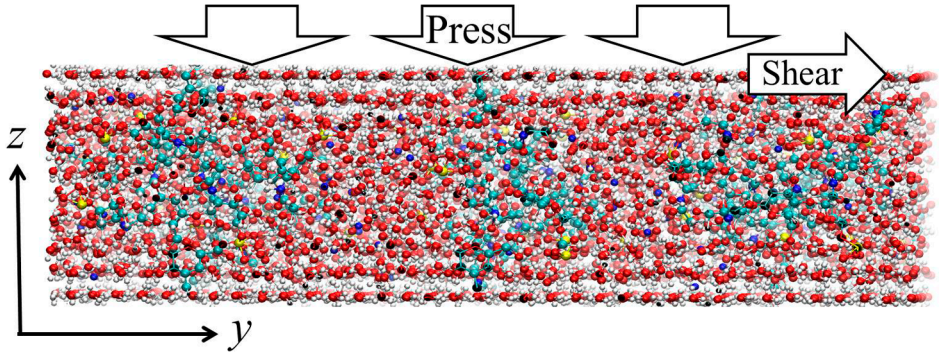


**Figure 2** A snapshot of the simulation system at equilibrium; side view of Model 2.

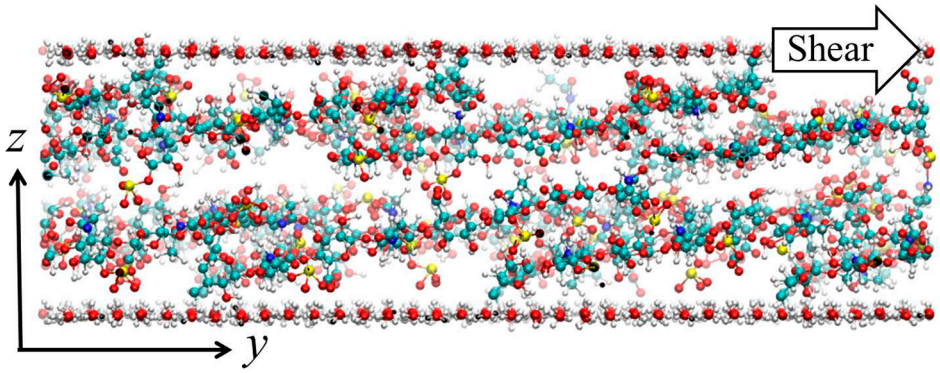


**Figure 3** Example of polymer conformation under constant shear; side view of Model 2. Only the polymers and the embedded water molecules are shown.

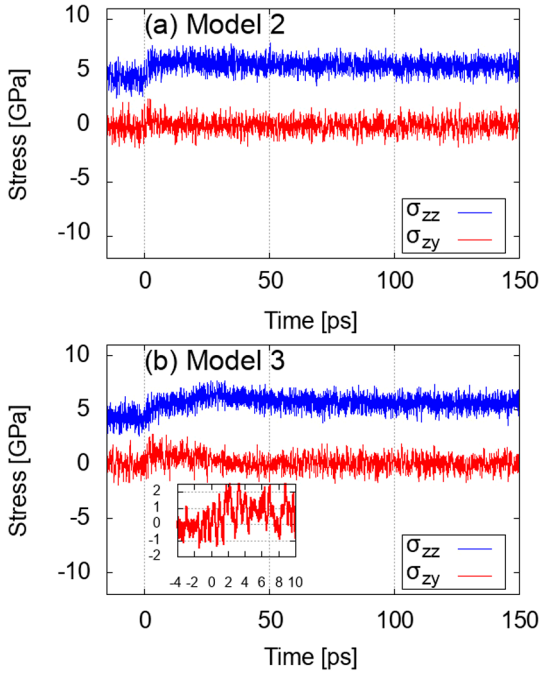


**Figure 4** Example of stress change during the simulation. Inserted is an enlarged figure for $\sigma_{zy}$ to show the increase after the sliding starts.

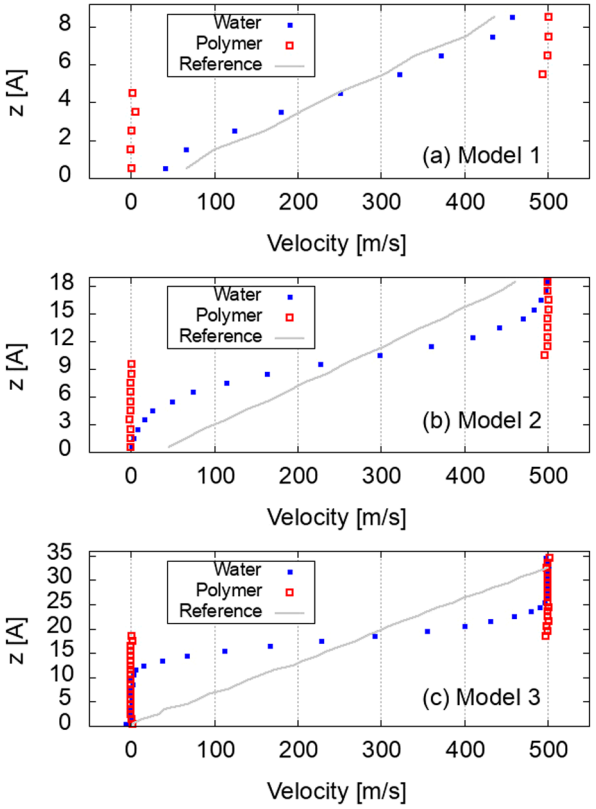


**Figure 5** Velocity profiles at the steady state. "Reference" is the profile of the pure water (without polymers) system with the same gap distance.

polymers are gradually elongated and the shear stress is relaxed to a steady state value. The relaxation time is longer for longer polymers. In the following analyses, we assume that Model 1 and Model 2 reach the steady state at 60 ps and Model 3 at 90 ps. Time average is taken for ~100 ps after reaching the steady state.

The mean values of $\sigma_{zz}$ and $\sigma_{zy}$ are shown in Table 2. Results for the system without polymers are shown as a reference (Model 0). For Model 3, simulation with higher shear rate ($v_0$=1000 m/s) was separately executed to investigate the shear rate dependence.

The dynamic friction coefficient $\mu_f$ is defined as

$$\mu_f = \frac{\langle \sigma_{zy} \rangle}{\langle \sigma_{zz} \rangle} \tag{3}$$

Two relevant factors exist, the polymer length and the shear rate. For longer polymers the friction coefficient drastically decreases; for example, $\mu_f \approx 0.01$ for Model 3, which is similar to experiments [2]. The shear rate dependence seems weak.

## Velocity profile

To look into the mechanism of friction reduction by grafted polymers, the velocity profile is investigated (Fig. 5). In the reference systems where the thin gap is filled only with water, the Couette flow is realized.

For the Couette flow, we can evaluate the viscosity coefficient $\mu_v$ of water as

$$\langle \sigma_{zy} \rangle = \mu_v \frac{v_0}{L} \tag{4}$$

We obtain $\mu_v = 2.61 \times 10^{-3}$ Pa·s, which is close to the experimental value of water at 298 K, $1.00 \times 10^{-3}$ Pa·s [23].

## Distribution of mass and charge

The density profile shown in Figure 6 gives another

**Table 2** Mean stress and friction coefficient

| | Sliding speed [m/s] | Shear rate [$10^9$ s$^{-1}$] | $\sigma_{zz}$ [GPa] | $\sigma_{zy}$ [GPa] | Friction coefficient [–] |
|---|---|---|---|---|---|
| Model 0 | 500 | 143 | 5.15±0.57 | 0.373±0.663 | $72.5 \times 10^{-3}$ |
| Model 1 | 500 | 556 | 4.81±0.54 | 0.535±0.570 | $111 \times 10^{-3}$ |
| Model 2 | 500 | 263 | 5.75±0.52 | 0.250±0.578 | $43.5 \times 10^{-3}$ |
| Model 3 | 500 | 143 | 5.57±0.52 | 0.0466±0.580 | $8.37 \times 10^{-3}$ |
| | 1000 | 286 | 5.78±0.43 | 0.0514±0.465 | $8.90 \times 10^{-3}$ |

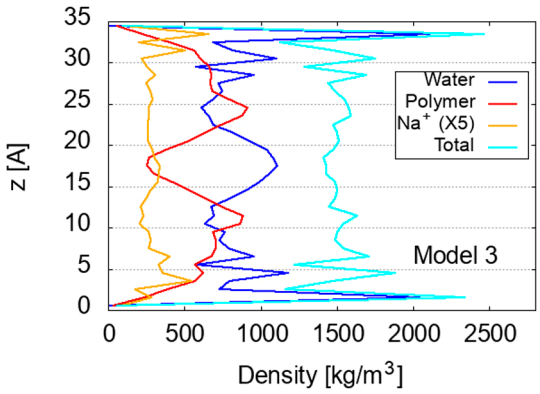


**Figure 6** Density profile at the steady state for Model 3. The profile of $Na^+$ is enlarged by five times.

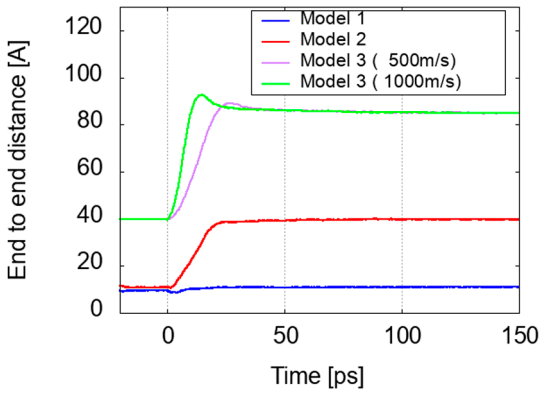


**Figure 8** Change of the end-to-end distance of the grafted polymers during the simulation.

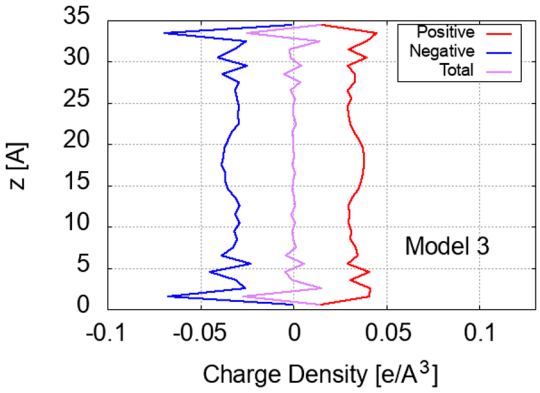


**Figure 7** Charge density profile at the steady state for Model 3. The unit of the charge density is $e/A^3$, where $e$ is the elementary charge.

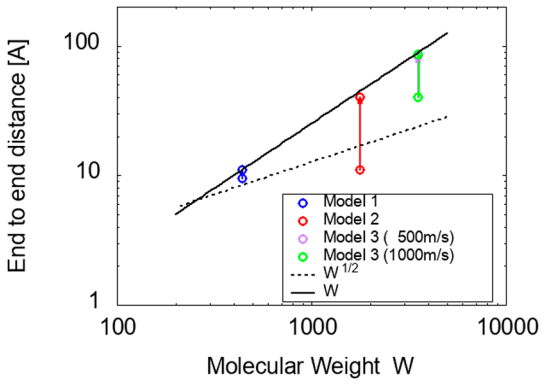


**Figure 9** End-to-end distance, changing from the equilibrium values to the steady state ones.

insight. As the polymers move with the surface, a large amount of water is pushed out to the central slipping region. The water density is also high near the surface due to surface adsorption. It is interesting to note that sodium ions also prefer the central water-rich region, suggesting large stabilization due to hydration.

The local density of electric charge, including partial charge as well as ionic one, is also investigated, as shown in Figure 7. Although small deviation exists, the charge neutrality holds in general, even under a large shear ($v_0$=500 m/s), and no electrokinetic phenomena, such as sedimentation potential, are observed. However, they may exist when extra electrolytes are added; the investigation is under way.

## Polymer deformation

A simple measure of polymer deformation is the end-to-end distance $R_e$ defined as

$$R_e = \langle |\vec{r}_N - \vec{r}_1| \rangle \quad (5)$$

where $\vec{r}_1$ and $\vec{r}_N$ are the atomic position of the graft point and the chain end, respectively. The change of $R_e$ is shown in Figure 8. At equilibrium $R_e$ is small. When the sliding starts, the grafted polymers elongate, leading to the $R_e$ increase to a steady value for the case of Model 2 and Model 3. An overshoot is observed for the longest polymer case (Model 3).

The transition from the equilibrium to the steady state is summarized in Figure 9 as a molecular weight ($W$) dependence. In the nature (equilibrium) state with a random coil shape, we expect $R_e \propto \sqrt{W}$ (dashed line), which roughly holds. The elongated state has $R_e \propto W$ as expected.

Detailed analysis in energetics (change in conformation and solvation) is described elsewhere, but only the total potential energy is shown in Figure 10. It increases soon after the sliding starts and reaches the steady value after an overshoot.

Here we give a brief comparison between our model and real joint systems. The typical chain length in the real system is 200–600 A [19] while that of our model is 75 A at most due to the computational resource limit. We have accordingly chosen a smaller gap distance (35 A). The characteristic time of the brush chain (e.g., the time for the chain to relax into equilibrium from a stretched form) is thus expected to be shorter than that of the real system. However, in the

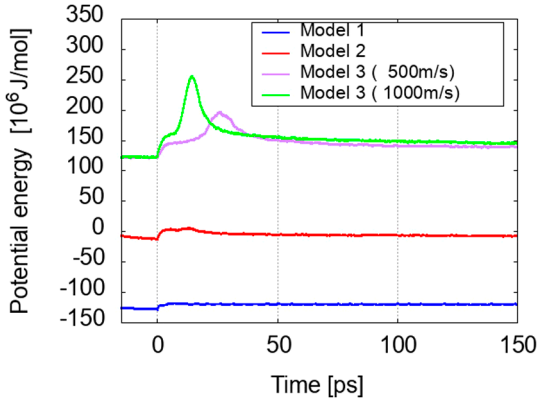


**Figure 10** Change of the total potential energy during the simulation.

lubrication properties investigated in this study, the polymer behaviour is mainly determined by the shear speed; the deformation time is inversely proportional to the shear speed, as shown in Figure 8, and the extrapolation to the real system conditions seems straightforward.

The difference in the shear rate seems to bring a more serious problem. The typical shear rate ranges in $10-10^3\ s^{-1}$ for the real system [3] while it is $\sim 10^{11}\ s^{-1}$ for our model (Table 2); the discrepancy in the shear rate is huge. However, in the boundary lubrication regime where both surfaces directly interact, the sliding speed is the relevant parameter, not the shear rate. Typical sliding speed in the real situation is 0.1−10 m/s; although our speed (500 or 1000 m/s) is still two orders of magnitude larger, it would be possible to extrapolate our results into ~10 m/s conditions.

## Conclusion

Molecular simulation is a useful tool to investigate the dynamics of various biological systems in microscopic scales. As an example, a nanoscale polymer model was proposed in this paper to study the role of polymer brush in joint lubrication. We found that the interaction between the biopolymers grafted on resilient surface and the surrounding synovial fluid causes a large modification from the Couette flow, leading to a drastic shear reduction and a friction coefficient decrease.

Although we have been forced to carry out the simulations under extreme conditions, such as shorter chains and larger shear rate, we expect that these findings are useful to study the lubrication mechanism in microscales.

There exist many relevant parameters, such as graft density, graft site arrangement (e.g., lattice-like or random), electrolyte concentration and other components (e.g., hyaluronic acid and glycoprotein) of synovial fluid. Investigation of their contribution is underway.

## Acknowledgement

We are grateful for Prof. N. Tomita and his laboratory members at Kyoto University for encouragement and stimulating discussion.

## Conflicts of Interest

The authors declare no conflicts of interest.

## Author Contribution

N. K. carried out the simulation and data analysis, and prepared the manuscript. M. M. was the principal investigator and co-wrote the manuscript.

## Reference

[1] Evans, E. G. *Studies on the anatomy and function of bone and joints* (Springer, Berlin, 2012).
[2] Mow, V. C. & Lai, W. M. Mechanics of animal joints. *Annu. Rev. Fluid Mech.* **11**, 247–288 (1979).
[3] Dowson, D. Bio-tribology. *Faraday Discuss.* **156**, 9–30 (2012).
[4] Greene, G. W., Olszewska, A., Osterberg, M., Zhu, H. & Horn, R. A cartilage-inspired lubrication system. *Soft Matter.* **10**, 374–382 (2014).
[5] Ateshian, G. A. The role of interstitial fluid pressurization in articular cartilage lubrication. *J. Biomech.* **42**, 1163–1176 (2009).
[6] Murakami, T., Higaki, H., Sawae, Y., Ohtsuki, N., Moriyama, S. & Nakanishi, Y. Adaptive multimode lubrication in natural synovial joints and artificial joints. *Proc. Inst. Mech. Eng. H* **212**, 23–35 (1998).
[7] Greene, G. W., Banquy, X., Lee, D. W., Lowrey, D. D., Yu, J. & Israelachvili, J. N. Adaptive mechanically controlled lubrication mechanism found in articular joints. *Proc. Natl. Acad. Sci. USA* **108**, 5255–5259 (2011).
[8] Klein, J. Polymers in living systems: From biological lubrication to tissue engineering and biomedical devices. *Polym. Adv. Technol.* **23**, 729–735 (2012).
[9] Ide, M. & Matsumoto, M. Tribology of polymer brush: Microscale modelling and simulation. *Mol. Simul.* **41**, 942–947 (2015).
[10] LAMMPS Molecular Dynamics Simulator. http://lammps.sandia.gov/
[11] Hockney, R. W. & Eastwood, J. W. *Computer simulation using particles* (McGraw-Hill international Book, Tokyo, 1981).
[12] Mayo, S. L., Olafson, B. D. & Goddard III, W. A. Dreiding: A generic force field for molecular simulations. *J. Phys. Chem.* **94**, 8897–8909 (1990).
[13] Jang, S. S. & Goddard III, W. A. Structures and transport properties of hydrated water-soluble dendrimer-grafted polymer membranes for application to polymer electrolyte membrane fuel cells: classical molecular dynamics approach. *J. Phys. Chem. C* **111**, 2759–2769 (2007).
[14] Jang, S. S., Goddard III, W. A. & Kalani, M. Y. S. Mechanical and transport properties of the poly(ethylene oxide)–poly(acrylic acid) double network hydrogel from molecular dynamics simulations. *J. Phys. Chem. B* **111**, 1729–1737 (2007).
[15] Lee, S. G., Brunello, G. F., Jang, S. S. & Bucknall, D. G. Molecular dynamics simulation study of P(VP-co-HEMA) hydrogels: effect of water content on equilibrium structures

and mechanical properties. *Biomaterials* **30**, 6130–6141 (2009).
[16] Jorgensen, W. L., Chandrasekhar, J. & Madura, J. D. Comparison of simple potential functions for simulating water. *J. Chem. Phys.* **78**, 926–935 (1983).
[17] Roughley, P. J. The structure and function of cartilage proteoglycans. *Eur. Cell Mater.* **12**, 92–101 (2006).
[18] Ng, L., Grodzinsky, A. J., Patwari, P., Sandy, J., Plass, A. & Ortiz, C. Individual cartilage aggercan macromolecules and their constituent glycosaminoglycans visualized via atomic force microscopy. *J. Struct. Biol.* **143**, 242–257 (2003).
[19] Mourao, P. A. S. Distribution of chondroitin 4-sulfate and chondroitin 6-sulfate in human articular and growth cartilage. *Arthritis Rheum.* **31**, 1028–1033 (1988).
[20] Hui, A. Y., McCart, W. J., Masuda, K., Firestein, G. S. & Sah, R. L. A systems biology approach to synovial joint lubrication in health, injury and disease. *Wiley Interdiscip. Rev. Syst. Biol. Med.* **4**, 15–37 (2012).
[21] Okada, I., Namiki, Y., Aizawa, M. & Itatani, K. MD simulation of crystal growth of NaCl from its supersaturated aqueous solution. *J. Mol. Liquids* **118**, 131–139 (2005).
[22] Cohen, N. P., Foster, R J. & Mow, V. C. Composition and dynamics of articular cartilage: Structure, function, and maintaining health state. *J. Orthop. Sports Phys. Ther.* **28**, 203–215 (1998).
[23] Lide, D. R. *CRC Handbook of Chemistry and Physics*, 72nd ed. (CRC Press, Boca Raton, 1991).